ADVANCES IN ATMOSPHERIC SCIENCES, VOL. 31, JANUARY 2014, 110–117

Variation Characteristics of Ultraviolet Radiation over the North China Plain

HU Bo* and WANG Yuesi

State Key Laboratory of Atmospheric Boundary Layer Physics and Atmospheric Chemistry,
Institute of Atmospheric Physics, Chinese Academy of Sciences, Beijing 100029

(Received 28 December 2012; revised 7 April 2013; accepted 22 April 2013)

ABSTRACT

In situ measured data of broadband solar radiation (R_s) and ultraviolet (U_v) radiation were used to investigate the spatiotemporal variation properties of U_v radiation and the ratio of U_v radiation to R_s over the North China Plain (NCP). Based on the analysis, an empirical model for estimating U_v radiation under all weather conditions in this region was developed. The results showed that the annual U_v radiation over the NCP ranges from 0.38–0.52 MJ m^{-2} d^{-1}. The highest value during the study period was recorded at the Changwu site, which is located near the margin of the Loess Plateau, while the lowest value appeared at the station in Beijing. The seasonal variation pattern of the ratio of U_v radiation to R_s is similar to that of U_v radiation; namely, the highest value appears in August and then decreases gradually until the lowest value appears in November. A small increasing trend in the U_v radiation levels and the ratio of U_v radiation to R_s was observed over the NCP. The evaluation results showed that the empirical estimation model can be widely used to estimate U_v radiation under all atmospheric conditions. The relative error between the modeled and measured daily values were within ±15%.

Key words: ultraviolet radiation, North China Plain, increasing trend, parameterization method

Citation: Hu, B., and Y. S. Wang, 2014: Variation characteristics of ultraviolet radiation over the North China Plain. *Adv. Atmos. Sci.*, **31**(1), 110–117, doi: 10.1007/s00376-013-2319-5.

1. Introduction

Ultraviolet (U_v) radiation is defined as the sum of UVB and UVA radiation. The solar spectrum ranging from 280–315 nm is defined as UVB radiation and that from 315–400 nm is termed UVA radiation. Research indicates that U_v radiation received at the surface of the Earth is 10% UVB and 90% UVA. Even at the top of the atmosphere, the percentage of U_v radiation to broadband solar radiation (R_s) is no more than 10%. So, the proportion of U_v radiation to R_s that reaches the Earth's surface is smaller than that at the top of the atmosphere. Many research results have shown that U_v radiation is an indispensable parameter in the study of environmental issues and ecological processes. Many adverse health and environmental effects can be caused by excessive U_v radiation doses [Slaper and Koskela, 1997; National Radiological Protection Board, 2002; United Nations Environment Programme (UNEP), 2003; Outer et al., 2005]. For instance, enhanced U_v radiation can delay the growth and development of plants. An especially excessive dose of UVB radiation can penetrate through the leaf epidermis, and thus may injure the photosynthetic system and cell membrane and disrupt phytohormones. Correspondingly, the photosynthetic capacity, biomolecules, biomass, and ecophysiological characteristics of plants and ecosystems may also be influenced by high UVB radiation doses. In general, excessive UVB radiation can modify DNA and protein structure, resulting in changes in physiological and biochemical processes. The properties of U_v radiation also need to be investigated to study tropospheric chemistry and oceanography, skin cancer and forest degradation (Grants and Heisler, 1997; McKenzie et al., 2001). Knowledge of long-term variation properties of U_v radiation is an important parameter for evaluating the health and environmental risks it causes (Slaper and Koskela, 1997; Cañda et al., 2000).

Early research noted that solar zenith angles, altitude, cloud micro-properties, concentration of the ozone column and the physico-chemical characteristics of aerosols have a strong influence on the variation characteristics of U_v radiation (Piazena, 1996; Seckmeyer et al., 1997; McKenzie et al., 2001). However, to meet the demands of studies on health risks and environmental problems, more detailed knowledge of U_v radiation was required. Thus, numerous further studies on the variation characteristics of U_v radiation and the ratio of U_v to R_s have also been carried out, and still need to be carried out. Many such studies have reported a number of different estimation methods that can be used to calculate historic U_v radiation under clear sky conditions (Foyo-Moreno et al., 2003; Paulescu et al., 2010). For instance, *in situ* observed and reconstructed U_v radiation data have been used to investigate the long-term variation trends of U_v radiation

* Corresponding author: HU Bo
E-mail: hbooo@163.com

(Kaurola et al., 2000; Fioletov et al., 2001; Lindfors et al., 2007; Feister et al., 2008; Hu et al., 2010). However, studies on the long-term variation characteristics of $U_{\rm v}$ radiation are very scarce, especially over the North China Plain (NCP).

To further understand the mechanisms of interaction between enhanced $U_{\rm v}$ radiation and the ecosystem, and to better prevent damage to plants and ecosystems caused by $U_{\rm v}$ radiation, larger-scale and long-term field research on $U_{\rm v}$ radiation should be carried out. However, the observer networks for $U_{\rm v}$ radiation are extremely scarce, particularly in the NCP. Thus, investigating the spatiotemporal variation characteristics of $U_{\rm v}$ radiation has great significance for agriculture, as the NCP is one of the most important agricultural regions of China.

In the above context, the goal of the present reported study—besides investigating the temporal variation characteristics of $U_{\rm v}$ and the ratio of $U_{\rm v}$ radiation to $R_{\rm s}$—was to present an efficient and accurate parameterization method for estimating $U_{\rm v}$ radiation through more routinely measured $R_{\rm s}$. The estimation model was validated, and the transferability of the model evaluated.

2. Materials and methods

2.1. *Site*

The NCP is known as China's "granary", as more than 40% and 25% of China's wheat and corn production is produced in this region, respectively (Zhang et al., 2010). The NCP is located in the Yellow River valley, and is the largest alluvial plain in eastern Asia. The northern and western parts of the NCP are surrounded by the Yanshan Mountains and the Taihang Mountains, respectively. In the southern part, the Yangtze Plain is situated adjacent to the NCP. The Bohai Sea, Shandong Peninsula and the Yellow Sea lie in the eastern part of the NCP. The vast majority of Henan, Hebei and Shandong provinces consist of the NCP. It covers an area of approximately 409 500 km^2 and the elevation of the majority of the region is less than 50 m. The NCP formed the cradle of Chinese civilization, and the region is among the most densely populated in the world. Six radiation observation stations were involved in this study and are affiliated with the Chinese Ecosystem Research Network (CERN) (Fig. 1).

$R_{\rm s}, U_{\rm v}$ radiation, photosynthetically active radiation, reflected radiation, net radiation and routine meteorological parameters are measured simultaneously by this observation network. The *in situ* measured $U_{\rm v}$ radiation and $R_{\rm s}$ data were used to investigate the variation characteristics of $U_{\rm v}$ radiation and the ratio of $U_{\rm v}$ radiation to $R_{\rm s}$ over the NCP region. Measured data from January 2005 to December 2011 were used in this study, with the exception of the Jiaozhouwan site due to its late installation.

2.2. *Instruments and data quality control*

A CM-11 radiometer (Kipp and Zonen, Delft, Netherlands) was used to measure $R_{\rm s}$, and the uncertainty of the measured $R_{\rm s}$ values was less than 3%. A CUV3 (Delft, Netherlands) was used to measure the sum of direct and scatter $U_{\rm v}$ radiation with a relative error less than 5%. An HMP45D apparatus (Vaisala, Finland) was used to measure the relative humidity (RH) and temperature. The measured accuracies for RH and temperature were 3% and 0.1°C, respectively. The solar radiation and meteorological parameters were observed at 1-minute intervals. The hourly and daily values were integrated from the minute data. All instruments were calibrated every two years. In addition, daily maintenance work was performed to ensure the radiometers were clear, free of dirt and positioned horizontally. Hu et al. (2010) reported a detailed description of the calibration method.

The control criteria employed for the measured $U_{\rm v}$ radiation data were as follows. First, the measured values of $U_{\rm v}$ radiation could not be higher than the flux value of the $U_{\rm v}$ radiation at the top of the atmosphere in the same geographical coordinates. Second, the ratio of $U_{\rm v}$ radiation to $R_{\rm s}$ had to range from 0.02 to 0.08. Otherwise, the measured $U_{\rm v}$ radiation data were deleted from the measured dataset. The quality control method for $R_{\rm s}$ was similar to that for U_v radia-

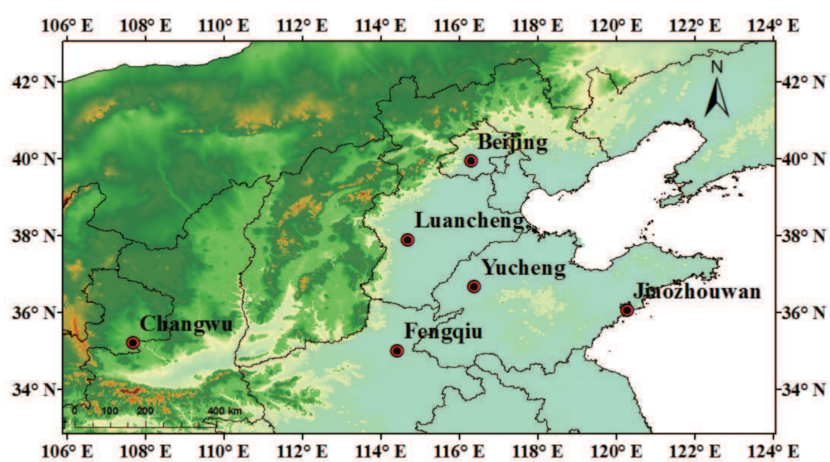

Fig. 1. Geographical locations of the observation sites in the NCP.

tion. First, the values of the measured R_s could not be higher than the values at the top of the atmosphere in the same geographical coordinates. Moreover, the minimum value of R_s that could be accepted had to be higher than the minimum value appearing in continuous overcast conditions; namely, the clearness index (the ratio of R_s to the extraterrestrial irradiance flux of R_s at the top of the atmosphere) had to be larger than 0.03. The value of 0.03 represents a continuous heavily overcast sky condition (Geiger et al., 2002). Otherwise, the measured R_s was deleted from the measured dataset. No more than 2% of the measured data were eliminated after the quality control procedure.

3. Results and discussion

3.1. *Temporal variation characteristics of* U_v *radiation*

Figure 2 shows box plots of the monthly statistics of U_v radiation over the NCP. We can see that the lowest value of U_v radiation appears in winter and the highest value in summer (June). An increasing trend of U_v radiation can be observed from winter to summer. The U_v radiation values then decrease gradually until reaching the minimum in winter. The monthly variation feature of the U_v radiation is similar to that of R_s. The variation characteristics of the solar zenith angle are mainly responsible for the type of monthly variation of the U_v radiation.

The annual average values of U_v radiation are 0.38, 0.43, 0.47, 0.51, 0.52 and 0.46 MJ m^{-2} d^{-1} at Beijing, Luancheng, Yucheng, Jiaozhouwan, Changwu and Fengqiu, respectively. The measured U_v radiation at the Beijing site was the lowest U_v value in the NCP region.

Beijing is capital of China and is one of the largest cities in the world. There are more than 14 million people in Beijing. The northern and western parts of Beijing are surrounding by the Yanshan Mountains and the Taihang Mountains, with elevations between 1000 and 3500 m above sea level. The southern and eastern parts of the city are adjacent to the NCP. There are many heavily industrialized areas from the southwest to the east (Streets et al., 2007). Air pollution is very severe in Beijing, especially atmospheric fine aerosol pollution. Rapid economic development, population expansion and urbanization are the main factors causing the heavy levels of air pollution in Beijing. Many research results have shown that fine aerosol particles are the main air pollutant. Recently, the concentration of $PM_{2.5}$ has also been found to be very high in Beijing (Chan and Yao, 2008; Zhao et al., 2011). As is known, fine particles can have a strong extinction effect on U_v radiation through selective scattering and absorption (Eck et al., 2005). A higher concentration of fine particles causes a greater abatement of short-wave radiation by scattering and absorption effects, so the lowest U_v radiation values appear in Beijing. A high concentration of column-integrated water vapor will increase attenuation of solar radiation. In contrast, fewer fine particles and less water vapor result in relatively high U_v radiation. This is based on the principle that the absorption of water vapor to the solar band is stronger than to the U_v band. The effects of fine particles and water vapor lead to the highest U_v radiation being observed at Changwu, which is situated near the margin of the Loess Plateau, and where there are much lower fine aerosol concentrations (Wang et al., 2008) and lower water vapor.

In the present study we focused on the station at Beijing due to the comprehensive measurements carried out there. As shown in Fig. 3, we can see that there is a smaller increasing trend. Moreover, there is a quasi-biennial oscillation of U_v radiation, mainly due to monsoon activity. The increasing trend of U_v radiation is mainly caused by the slightly decreasing amounts of ozone and fine aerosols in the recent period. The ozone data were obtained from TOMS (http://toms.gsfc.nasa.gov/). The total amount of ozone over

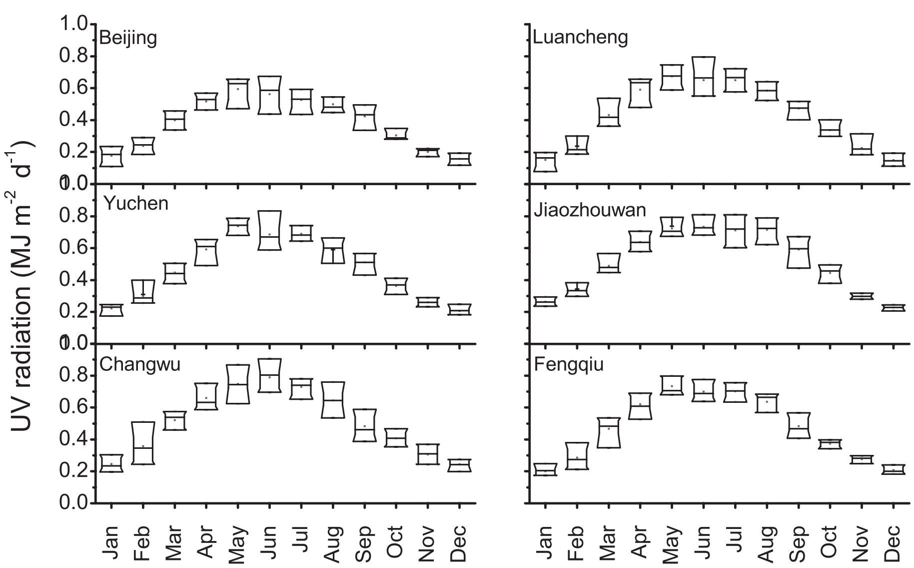

Fig. 2. Box plots of monthly ultraviolet radiation over the NCP.

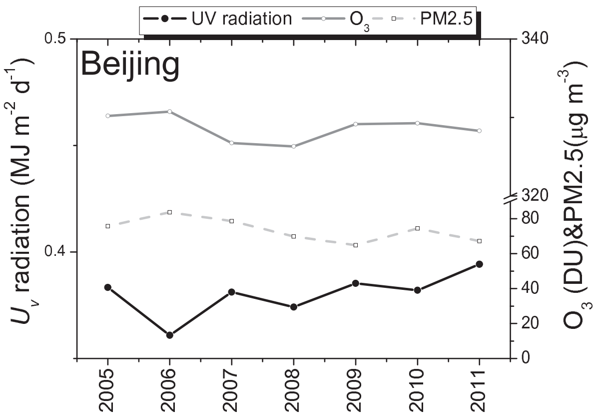

Fig. 3. Annual variations of U_v vs. the total values of ozone and the concentration of PM2.5 at the Beijing site.

Beijing decreased from 330 DU in 2005 to 228 DU in 2011. This decreasing trend of total ozone can also be seen at all other observation sites in the NCP region. Furthermore, the concentration of fine aerosol (PM2.5) in Beijing decreased from 83 μg m^{-3} in 2005 to 67 μg m^{-3} in 2011. A lower extinction effect of ozone and aerosol on short wavelength solar radiation results in higher U_v radiation.

3.2. *Variation characteristics of daily average* U_v/R_s

Many studies have been carried out to obtain more U_v radiation data based on the relationship between simultaneous observation values of U_v radiation and R_s (Barbero et al., 2006; Mateos-Villán et al., 2010). The climatic variation characteristics of U_v radiation and the effect of U_v radiation on ecology are investigated using these long-term U_v radiation data. The U_v radiation estimation method obtains the relationship between U_v radiation and R_s through a linear regression process. Based on this linear relationship, the history of U_v radiation is calculated from more routinely measured R_s data. However, the ratio of U_v to R_s must be recalibrated according to local climate conditions and geography (Udo, 2000). The spatiotemporal variation properties of the ratio of U_v radiation to R_s are very useful for studying the long-term variation characteristics of U_v radiation, especially for sites without *in situ* measurement data of U_v radiation. The monthly variation properties of the ratio of U_v radiation to R_s are shown in Fig. 4. From this figure, we can see there is an obvious seasonal variation feature of this ratio. There is a gradually increasing trend of this ratio from April until the highest values appear in summer (August). Then, there is a gradual decrease until the lowest values appear in winter. The seasonal variation trend of this ratio is caused by the seasonal variation feature of water vapor content (Fig. 4). As is well known, the NCP is mainly influenced by the East Asian monsoon. In general, water vapor increases from spring until a maximum value appears in summer caused by enriched rainfall in this period. From August, water vapor starts to decrease gradually, due to the withdrawal of the monsoon. In theory, water vapor has a stronger extinction effect on the solar band than the U_v band.

The spatial distribution of the ratio of U_v radiation to R_s is shown in Table 1. The range of this ratio varies from 0.031 ± 0.004 to 0.42 ± 0.006 over the NCP. As expected, the highest values of this ratio were recorded at the Jiaozhouwang site due to the higher content of water vapor and low $PM_{2.5}$ concentration in the atmosphere (Table 1). Results have indicated that there is heavy aerosol loading in coarse-mode particles due to the humidity-swelling of sea salt aerosols, so the abatement effect of $PM_{2.5}$ on U_v radiation is relatively small (Wang et al., 2008). The Jiaozhouwan site is located on the Shandong Peninsula, and is well known for its monsoon-influenced climate. Temperature and precipitation measurements classify this site as "intermediate humid subtropical" and "humid continental", respectively.

The lowest value of the ratio of U_v radiation to R_s was observed at Beijing due to the highest fine aerosol concentrations and the relatively low RH. Beijing is located within the Beijing–Tianjin–Hebei (BTH) mega-city cluster. Air pollution in the BTH region has recently been very severe due to rapid economic development, population expansion and urbanization. Aerosol pollution—especially the concentration of $PM_{2.5}$—is more serious (Parrish and Zhu, 2009) in Beijing. The annual average concentration of $PM_{2.5}$ is higher than 101 mg m^{-3} (He et al., 2001; Zheng et al., 2005).

The physical foundation is that the extinction of aerosol particles is negatively related with wavelength. So the extinction to U_v radiation is more than to R_s. The water vapor absorption of the U_v band is smaller than the solar band, so the observed U_v radiation is almost constant and R_s decreases with increasing water vapor. Figure 4 shows a small increasing trend of the ratio of U_v radiation to R_s in this region due to the decreasing fine aerosol and increasing water vapor con-

Table 1. Annual average daily U_v radiation (MJ m^{-2} d^{-1}) and ratio of U_v radiation to R_s over the NCP.

Observation Site	Lat.	Lon.	Altitude	U_v	Ratio of U_v radiation to R_s	Column-integrated water vapor
Beijing	39°56'N	116°17'E	75 m	0.38 ± 0.16	0.031 ± 0.004	1.36 ± 1.06
Luancheng	37°53'N	114°41'E	50 m	0.43 ± 0.20	0.035 ± 0.009	1.65 ± 1.18
Yuchen	36°40'N	116°22'E	21 m	0.47 ± 0.19	0.037 ± 0.005	1.88 ± 1.26
Jiaozhouwan	36°03'N	120°16'E	6.8 m	0.51 ± 0.19	0.042 ± 0.006	1.94 ± 1.15
Changwu	35°12'N	107°40'E	1120 m	0.52 ± 0.20	0.040 ± 0.006	1.35 ± 0.85
Fengqiu	35°00'N	114°24'E	67 m	0.46 ± 0.22	0.040 ± 0.006	1.92 ± 1.19

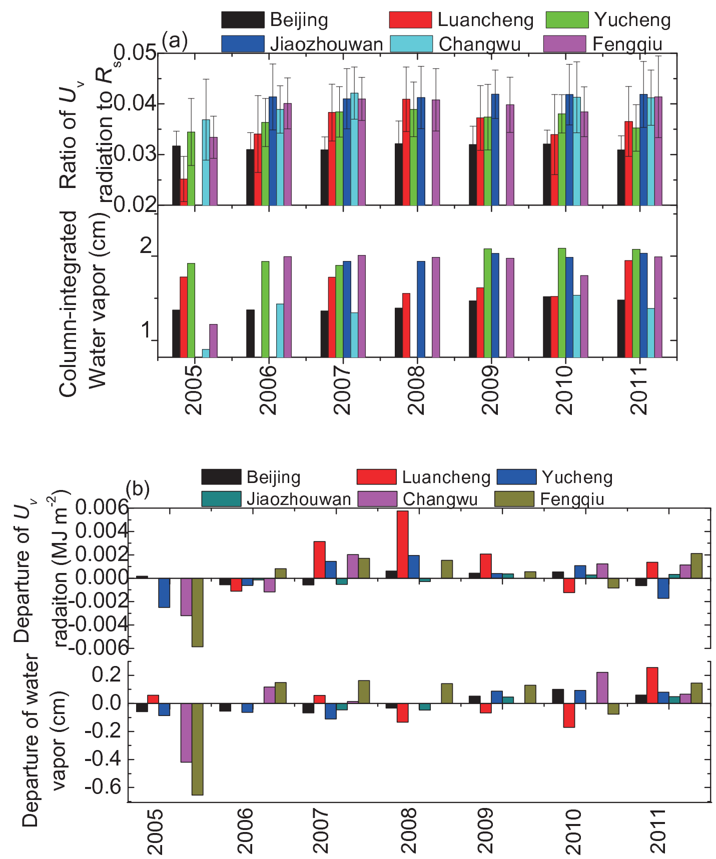

Fig. 4. Variation characteristics of U_v/R_s vs. column-integrated water vapor during the 2005–11 period over the NCP: (a) annual and (b) departure variation.

centration during the observation period.

3.3. *Effect of the clearness index on the ratio of U_v radiation to R_s*

Numerous factors can influence the amount of U_v radiation reaching the Earth's surface, such as solar altitude, the ozone column, aerosol concentrations, and microphysical aerosol and cloud properties. Altitude is another factor that can greatly influence U_v radiation (Piazena, 1996; Seckmeyer et al., 1997; McKenzie et al., 2001).

The extinction effect of clouds on U_v radiation depends on the microphysical characteristics of clouds, such as cloud cover, cloud level, cloud optical thickness, cloud water content, and cloud droplet spectra. To investigate the influence of clouds on U_v radiation, microphysical chemical parameters of clouds, such as cloud cover, level, type, and albedo, are necessary (Nemeth et al., 1996; Díaz et al., 2000; Foyo-Moreno et al., 2003). Unfortunately, these parameters are difficult to obtain due to the high degree of variability of clouds.

Many studies have indicated that the clearness index (K_s) can be used as a general indicator for extinction effect processes caused by aerosols, gases and clouds during the transfer of solar radiation through the atmosphere (Liu and Jordan, 1960). Accordingly, this parameter was used instead of cloud parameters. K_s was also used to analyze the influence of clouds on the ratio of U_v radiation to R_s. The definition of K_s is the ratio of R_s that reaches the surface to the solar irradiance flux at the top of the atmosphere.

Figure 5 shows opposite variation features of K_s compared with the ratio of U_v radiation to R_s. Minimum K_s values occur in the rainy season (i.e., the summer period), which indicates higher extinction causes higher water concentration; namely, more clouds appear at this time. In contrast, a high K_s indicates low fine aerosols and water vapor, resulting in a small ratio due to a small abatement effect on shortwave solar radiation; namely, U_v radiation.

3.4. *Evaluation of a parameterization model for estimating U_v radiation in the NCP*

As mentioned above, non-dimensional parameters are influenced less by local features, so a parameterization estimation model for U_v radiation was developed based on K_s and the solar zenith angle with high accuracy (Foyo-Moreno et al., 2003; Varo et al., 2005; Barbero et al., 2006; Hu et al., 2010; Mateos Villán et al., 2010). Xia et al. (2008) reported that a power law equation can be used to describe the influence of the cosine of the solar zenith angle (μ) on U_v radiation. The power law equation for U_v radiation within a

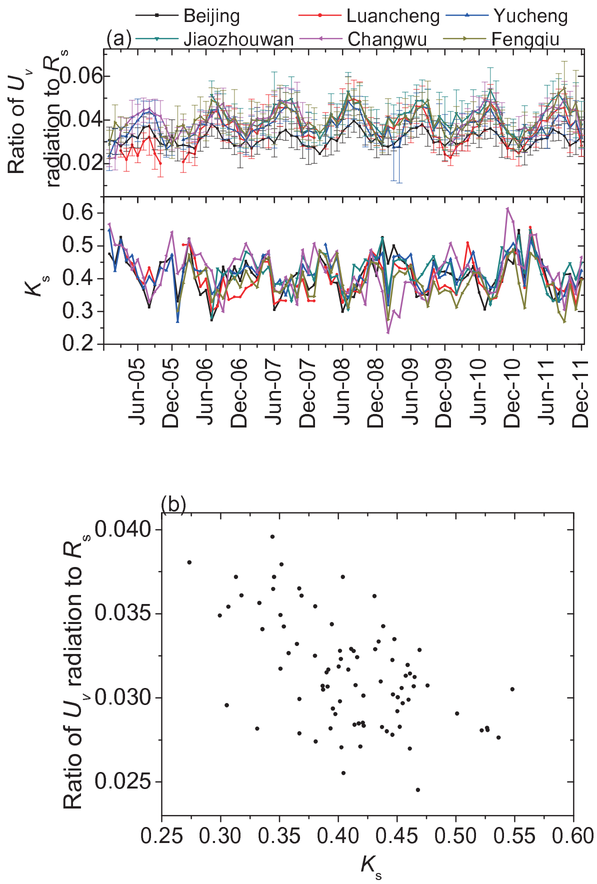

Fig. 5. Monthly daily average of $U_\mathrm{v}/R_\mathrm{s}$ and K_s in the NCP region: (a) temporal variation and (b) scatter plot of $U_\mathrm{v}/R_\mathrm{s}$ and K_s at Beijing Station.

narrow range of K_t can be written as

$$U_\mathrm{v} = U'_{\mathrm{v}0} \times \mu^N , \quad (1)$$

where $U'_{\mathrm{v}0}$ is the maximum value of U_v radiation per unit of μ. N determines how U_v changes with μ. Xia et al. (2008) also reported that the relationship between K_s and the maximum value of U_v radiation can be described by a polynomial equation. Hu et al. (2010) used measured data from 2005–08 in Beijing to develop a parametric equation to calculate the maximum value of U_v radiation based on K_s:

$$U'_{\mathrm{v}0} = 0.95 + 74K_\mathrm{s} - 74K_\mathrm{s}^2 + 55K_\mathrm{s}^3 , \quad (2)$$

A parameterization model for estimating U_v radiation based on the maximum value of U_v radiation and μ can be obtained. Xia et al. (2008) found that their equation [Eq. (1)] could obtain the U_v radiation highly accurately in Xianghe when parameter N is set as 1.06. Xianhe belongs to Hebei Province, which is located between two megacities, Beijing and Tianjin, 70 km to the northwest and to the southeast, respectively. According to Xia et al. (2008), we set parameter N as 1.06 in the parameterization model for estimating U_v radiation developed for the Beijing site.

$$U_\mathrm{v} = (0.95 + 74K_\mathrm{s} - 74K_\mathrm{s}^2 + 55K_\mathrm{s}^3) \times \mu^{1.06} . \quad (3)$$

The evaluated results indicate that this parameterization model can obtain a more accurate estimation of U_v radiation from more routinely measured R_s data. Only solar elevation angle and cloudiness index parameters are involved in this parameterization estimation model. Furthermore, these two parameters can be easily obtained through more routinely observed data.

To test the transferability of the parameterization model, Eq. (3) was used to model hourly U_v radiation data through highly accurate measured R_s datasets collected at five other sites in the NCP. As shown in Table 2, the statistical parameters of the linear regression equation between the observed and modeled U_v radiation data show that this parameterization model can obtain accurate U_v radiation through the measured R_s datasets. The slope and intercept of the linear regression are close to 1 and 0, respectively. The relative deviations between the modeled and observed daily U_v radiation are less than 15%. The mean bias errors (MBEs) are −0.04, −0.02, 0.01, 0.04, and −0.01 MJ m^{-2} d^{-1}, for Luancheng, Yuchen, Jiaozhouwan, Changwu, and Fengqiu, respectively. The root mean square errors (RMSEs) are 0.08, 0.06, 0.08, 0.08, and 0.07 MJ m^{-2} d^{-1}, for Luancheng, Yuchen, Jiaozhouwan, Changwu, and Fengqiu, respectively. These results indicate that this parameterization model can be used to estimate U_v radiation at observation sites in the NCP region other than Beijing, where the estimation model was developed.

Table 2. Statistical parameters of linear regression between modeled and observed daily U_v radiation (MJ m^{-2}d^{-1}) over the NCP.

Observation Site	a	b	C^2	MBE	RMSE	Relative error (%)
Beijing	0.98	−0.009	0.94	−0.01	0.04	6.5
Luancheng	1.02	0.01	0.92	−0.04	0.08	13.3
Yuchen	1.02	0.0	0.93	−0.02	0.06	13.1
Jiaozhouwan	1.02	−0.05	0.92	0.01	0.08	13.6
Changwu	0.98	−0.05	0.93	0.04	0.08	13.8
Fengqiu	0.98	−0.01	0.92	−0.01	0.07	13.9

Note: Relative error(%) $= \dfrac{\sum_n |O_i - P_i|/O_i}{n} \times 100\%$. a, slope of the linear regression equation; b, intercept of the linear regression equation; C, correlation parameter; O_i, observed U_v radiation; P_i, modeled U_v radiation; n, number of observed data.

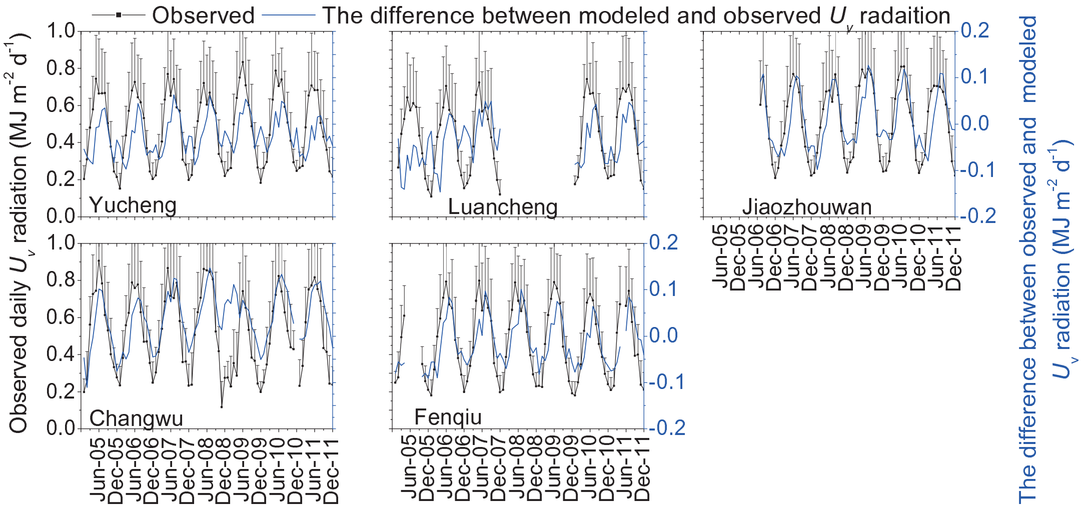

Fig. 6. Temporal variation characteristics of measured and model-predicted U_v radiation values in the NCP region.

The temporal variation characteristics of observed and modeled data are shown in Fig. 6. The same variation features of the modeled U_v radiation can be seen in the U_v radiation in Fig. 6, which indicates that the parameterization model can be used to calculate U_v radiation from the R_s dataset with high accuracy.

The advantage of this parameterization model is that it involves the cosine of the solar zenith angle and the measurement data of R_s. These two parameters can be obtained more easily because R_s is a routinely measured parameter in weather observation stations. However, there is a weakness in the parameterization model when transferred to other locations, especially for the relative deviation parameter. The results of Zerefos (2002) indicate that the total ozone concentration has a stronger influence on UVB than UVA under clear skies, so the effect of ozone on U_v radiation is not involved in this parameterization model. However, the effect of ozone on U_v radiation should be considered in further studies. This parameterization model can be easily modified to calculate daily U_v radiation with daily R_s by using the length of daytime, the daily average cosine of the solar zenith angle, and K_s.

4. Conclusions

The spatiotemporal variation properties of U_v radiation and the ratio of U_v radiation to R_s were analyzed in this study using in situ measurement data of U_v radiation and R_s from 2005–11 at six observation stations located in the NCP. The results showed that U_v radiation presents a similar seasonal variation to that of solar activity; that is, the values of U_v radiation gradually increase from spring until the highest values appear in summer, after which they decrease until the lowest values appear in winter. The highest value of U_v radiation was found to be 0.52 ± 0.20 MJ m^{-2} d^{-1}, recorded at the Changwu site. The lowest column-integrated water vapor and fewer fine particles at this site are the main factors leading to the highest values. In contrast, the strong extinction effect caused by the high fine aerosol burden results in the lowest value (0.53 ± 0.22 MJ m^{-2} d^{-1}), as measured at the Beijing site.

The average of the ratio of U_v radiation to R_s was found to range from 0.031 ± 0.004 to 0.042 ± 0.006 in the NCP region. The temporal variation characteristics of this ratio are the same as the U_v radiation. A high value appears in summer, and a low value appears in winter, with this variation pattern mainly being influenced by water vapor. The highest value of this ratio was observed at Jiaozhouwan due to the high water vapor and lower fine aerosol. A slight increasing trend of U_v radiation was discovered, and the ratio of U_v radiation to R_s in this region is caused by the decreasing trend of the concentration of fine aerosol and ozone and the increasing trend of water vapor.

A parameterization model was developed through the measured dataset of the Beijing observation site. This model was evaluated using measured data collected at the Beijing site and five other stations in the NCP. The regression results showed that this parameterization model can be used to obtain more accurate U_v radiation data from routinely measured R_s data. These results can provide more information for studying U_v radiation and climate change in the NCP region. Moreover, the parameterization model can improve the accuracy of estimating U_v radiation from R_s on a larger scale than that of only using the relationship between U_v radiation and R_s.

Acknowledgements. This work was supported financially by the National Natural Science Foundation of China (Grant Nos. 41275165 and 41230642) and the Research Program for excellent Ph.D. dissertations in the Chinese Academy of Sciences. The authors thank Dr. TANG Guiqian for drawing Fig. 1. The authors would also like to thank the CERN observation team for their *in situ* maintenance work.

REFERENCES

Barbero, F. J., G. Lopez, and F. J. Batlles, 2006: Determination of daily solar ultraviolet radiation using statistical models and artificial neural networks. *Ann. Geophys.*, **24**, 2105–2114.

Cañda, J., G. Pedrós, A. López, and J. V. Boscá, 2000: Influences of the clearness index for the whole spectrum and of the relative optical air mass on UV solar irradiance for two locations in the Mediterranean area, Valencia and Cordoba. *J. Geophys. Res.*, **105**, 4659–4766.

Chan, C. K., and X. Yao, 2008: Air pollution in mega cities in China. *Atmos. Environ.*, **42**, 1–42.

Díaz, S., G. Deferrari, D. Martinioni, and A. Oberto, 2000. Regression analysis of biologically effective integrated irradiances versus ozone, clouds and geometric factors. *Journal of Atmospheric and Solar-Terrestrial Physics*, **62**, 629–638.

Eck, T. F., and Coauthors, 2005: Columnar aerosol optical properties at AERONET sites in central eastern Asia and aerosol transport to the tropical mid-Pacific. *J. Geophys. Res.*, **110**, D06202, doi: 10.1029/2004JD005274.

Feister, U., J. Junk, and M. Woldt, 2008: Long-term solar UV radiation reconstructed by Artificial Neural Networks (ANN). *Atmos. Chem. Phys. Discuss*., **8**, 453–488.

Fioletov, V. E., L. McArthur, J. B. Kerr, and D. I. Wardle, 2001: Longterm variations of UV-B irradiance over Canada estimated from Brewer observations and derived from ozone and pyranometer measurements. *J. Geophys. Res.*, **106**, 23009–23028

Foyo-Moreno, I., I. Alados, F. J. Olmo, and L. Alados-Arboledas, 2003: The influence of cloudiness on UV global irradiance (295–385 nm). *Agricultural and Forest Meteorology*, **120**, 101–111.

Geiger, M., L. Diabaté, L. Ménard, and L. Wald, 2002: A web service for controlling the quality of measurements of global radiation. *Solar Energy*, **73**(6), 475–480.

Grants, R. H., and G. M. Heisler, 1997: Obscured overcast sky radiance distributions for ultraviolet and photosynthetically active radiation. *J. Appl. Meteorol.*, **36**, 1336–1345.

He, K. B., F. M. Yang, Y. Ma, Q. Zhang, X. Yao, C. K. Chan, S. Cadle, T. Chan, and P. Mulawa, 2001: The characteristics of PM2.5 in Beijing, China. *Atmos. Environ.*, **35**, 4959–4970.

Hu, B., Y. S. Wang, and G. R. Liu, 2010: Variation characteristics of ultraviolet radiation derived from measurement and reconstruction in Beijing, China. *Tellus B*, **62B**, 100–108.

Kaurola, J., P. Taalas, T. Koskela, J. Borkowski, and W. Josefsson, 2000: Long-term variations of UV-B doses at three stations in northern Europe. *J. Geophys. Res.*, **105**, 20813–20820.

Lindfors, A., J. Kaurola, A. Arola, T. Koskela, K. Lakkala, W. Josefsson, J. A. Olseth, and B. Johnsen, 2007: A method for reconstruction of past UV radiation based on radiative transfer modeling: Applied to four stations in northern Europe. *J. Geophys. Res.*, **112**, D23201, doi: 10.1029/2007JD008454.

Liu, B. Y. H., and R. C. Jordan, 1960: The interrelationship and characteristic distribution of direct, diffuse and total solar radiation. *Solar Energy*, **4**, 1–19.

Mateos-Villán, N. D., A. De Miguel-Castrillo, and J. Billbao Santos, 2010: Empirical models of UV total radiation and cloud effect study. *Inter J. Climatol.*, **30**, 1407–1415.

McKenzie, R. L., P. V. Johnston, D. Smale, B. A. Barry, and S. Madronich, 2001: Altitude effects on UV spectral irradiance deduced from measurements at Lauder, New Zealand, and at Mauna Loa Observatory, Hawaii. *J. Geophys. Res.*, **106**, 22845–22860.

National Radiological Protection Board, 2002: Health effects from ultraviolet radiation: Report of an advisory group on non-ionising radiation. Vol. 13, NO. 1, *Document of the National Radiological Protection Board*, Chilton. U. K., 279pp.

Nemeth, P., Z. Toth, and Z. Nagy, 1996. Effect of weather conditions on UV-B radiation reaching the earth's surface. *Journal of Photochemistry and Photobiology B: Biology*, **32**, 177–181.

Outer, K., P. N. Den, H. Slaper, and R. B. Tax, 2005: UV radiation in the Netherlands: Assessing long-term variability and trends in relation to ozone and clouds. *J. Geophys. Res.*, **110**, D02203, doi: 10.1029/2004JD004824.

Parrish, D. D., and T. Zhu, 2009: Clean air for megacities. *Science*, **326**(5953), 674–675, doi: 10.1126/science.1176064.

Paulescu, M., N. Stefu, E. Tulcan-Paulescu, D. Calinoiu, A. Neculae, and P. Gravila, 2010: UV solar irradiance from broadband radiation and other meteorological data. *Atmospheric Research*, **96**, 141–148.

Piazena, H., 1996: The effect of altitude upon the solar UV-B and UV-A irradiance in the topical Chilean Andes. *Solar Energy*, **57**, 133–140.

Seckmeyer, G., B. Mayer, G. Bernhard, A. Albold, R. Erb, H. Jaeger, and W. R. Stockwell, 1997: New maximum UV irradiance levels observed in central Europe. *Atmos. Environ.*, **31**, 2971–2976.

Slaper, H., and T. Koskela, 1997: Methodology of intercomparing spectral sky measurements, correcting for wavelength shifts, slit function differences and defining a spectral reference. *The Nordic Intercomparison of Ultraviolet and Total Ozone Instruments at Izana, October* 1996, Kjeldstad et al., Eds., Finn. Meteorol. Inst., Helsinki, 89–108.

Streets, D. G., and Coauthors, 2007: Air quality during the 2008 Beijing Olympic Games. *Atmos. Environ.*, **41**, 480–492.

Udo, S., 2000: Sky conditions at Ilorin as characterized by clearness index and relative sunshine. *Solar Energy*, **69**, 45–53.

United Nations Environment Programme (UNEP), 2003: Environmental effects of ozone depletion and its interactions with climate change: 2002 Assessment. Nairobi, Kenya, 177 pp.

Varo, M., G. Pedros, and P. Martinez-Jimenez, 2005: Modelling of broad band ultraviolet clearness index distributions for Cordoba, Spain. *Agriculture and Forest Meteorology*, **135**, 346–351.

Wang, Y. S., and Coauthors, 2008: Seasonal variations in aerosol optical properties over China. *Atmos. Chem. Phys. Discuss.*, **8**, 8431–8453.

Xia, X., Z. Li, P. Wang, M. Cribb, H. Chen, and Y. Zhao, 2008: Analysis of relationships between ultraviolet radiation (295–385 nm) and aerosols as well as shortwave radiation in North China Plain. *Ann. Geophys.*, **26**, 2043–2052

Zerefos, C. S., 2002: Long-term ozone and UV variations at Thessaloniki, Greece. *Phys. Chem. Earth*, **27**, 455–460.

Zhang, Y., A. J. Dore, L. Ma, X. J. Liu, W. Q. Ma, J. N. Cape, and F. S. Zhang, 2010: Agricultural ammonia emissions inventory and spatial distribution in the North China Plain. *Environment Pollution*, **158**, 490–501.

Zhao, X. J., X. L. Zhang, W. W. Pu, W. Meng, and X. F. Xu, 2011: Scattering properties of the atmospheric aerosol in Beijing, China. *Atmospheric Research*, **101**,799–808.

Zheng, M., L. G. Salmon, J. J. Schauer, L. M. Zeng, C. S. Kiang, Y. H. Zhang, and G. R. Cass, 2005: Seasonal trends in PM2.5 source contributions in Beijing, China. *Atmos. Environ.*, **39**, 3967–3976.